JAERI- M
9 7 8 8

MAJOR DISRUPTION PROCESS IN TOKAMAK

November 1 9 8 1

Gen-ichi KURITA, Masafumi AZUMI, Takashi TUDA,
Tomonori TAKIZUKA, Toshihide TSUNEMATSU,
Shinji TOKUDA, Kimitaka ITOH and Tatsuoki TAKEDA

日 本 原 子 力 研 究 所
Japan Atomic Energy Research Institute

JAERI-M 9788

Major Disruption Process in Tokamak

Gen-ichi KURITA, Masafumi AZUMI, Takashi TUDA, Tomonori TAKIZUKA
Toshihide TSUNEMATSU, Shinji TOKUDA, Kimitaka ITOH and
Tatsuoki TAKEDA

Division of Thermonuclear Fusion Research,
Tokai Research Establishment, JAERI

(Received October 20, 1981)

The major disruption in a cylindrical tokamak is investigated by using the multi-helicity code, and the destabilization of the 3/2 mode by the mode coupling with the 2/1 mode is confirmed. The evolution of the magnetic field topology caused by the major disruption is studied in detail. The effect of the internal disruption on the 2/1 magnetic island width is also studied. The 2/1 magnetic island is not enhanced by the flattening of the q-profile due to the internal disruption.

Keywords: Major Disruption, Tokamak, MHD Stability, Multi-helicity Code,
Magnetic Island Overlapping, Effect of Mode Coupling,
Effect of Internal Disruption

トカマクのメイジァ・ディスラプション過程

日本原子力研究所東海研究所核融合研究部

栗田源一・安積正史・津田　孝・滝塚知典
常松俊秀・徳田伸二・伊藤公孝・竹田辰興

（１９８１年１０月２０日受理）

円柱近似モデルでのメイジァ・ディスラプションについて３次元非線形コードを使って調べた。その結果，m／n=3／2モードが2／1モードとの結合により不安定になることがメイジァ・ディスラプションの原因になっていることがわかり，更に，磁場配位の非線形領域での変化について詳細な解析を行った。また，２／１モードが成長する機構を解明するために，インターナル・ディスラプションの２／１モードに対する影響を調べた。

Contents

目　　次

1. Introduction

The major disruption of a tokamak is characterized by rapid release of magnetic and plasma energies within an order of μs followed by reduction of the plasma current with the decay time of several milliseconds, and it is considered to be the main cause of limitation of the plasma current and density. The disruption may bring about a more serious damage to the device as the device becomes larger. It is, therefore, urgently required to clarify the mechanism of the major disruption and to devise methods to control or suppress it.

The m=2 tearing mode plays an important role in the major disruption. The growth of the m=2 magnetic field perturbation is observed as a precursor of the disruption. When the safty factor at plasma boundary, q_a, is less than 2, the major disruption seems to be suppressed. Waddell et al. proposed that a nonlinear interaction between m/n=2/1 and m/n=3/2 tearing modes causes the major disruption[1~4]. The results of their simulation seem to well recover the experimental data. They presented the scaling law of the major disruption time on the basis of the WKB theory. The WKB method, however, is not always applicable to the nonlinear stage of the mode evolution. It is important to establish the theoretical model reliable in this stage. It is also very important to know the mechanism to change the current profile which makes the enhancement of the 2/1 island width.

In this paper we first recover the results of the ORNL group. We find a little disagreement with their results. We also investigate the initiation process of the 2/1 mode assuming that the current density profile is flattened by the 1/1 mode. The 2/1 island obtained in the simulation is compared with those calculated by the Δ' code.

In the next section the basic equations of the present analysis are described. In §3, the results of simulation are presented. Conclusion and discussion are given in §4.

2. Basic Equations

The reduced set of the resistive magnetohydrodynamic equations of a low β toroidal plasma in the cylindrical coodinate system (R, Φ, z) is given as

$$\frac{\partial \Psi}{\partial t} + \vec{v} \cdot \vec{\nabla}_{\perp} \Psi = B_0 \frac{\partial \Phi}{\partial \zeta} + \eta J - E_w(t) \tag{1}$$

$$\frac{\partial U}{\partial t} + \vec{v} \cdot \vec{\nabla}_{\perp} U = \vec{\nabla}\zeta \cdot \vec{\nabla} P \times \vec{\nabla}_{\perp} \left(\frac{R}{R_0}\right)^2 + \left(\frac{R}{R_0}\right)^2 \vec{\nabla}\zeta \cdot \vec{\nabla}_{\perp} \Psi \times \vec{\nabla}_{\perp} J + B_0 \frac{\partial J}{\partial \zeta} \tag{2}$$

$$\frac{\partial P_*}{\partial t} + \vec{v} \cdot \vec{\nabla}_{\perp} P_* = 0 \tag{3}$$

$$\vec{B} = B_0 \left(\vec{\nabla}\zeta + \vec{\nabla}\zeta \times \vec{\nabla}_{\perp} \Psi \right) \tag{4}$$

$$\vec{v} = \left(\frac{R}{R_0}\right)^2 \vec{\nabla}\zeta \times \vec{\nabla}_{\perp} \Phi \tag{5}$$

$$\vec{J} = \left(R^2 \vec{\nabla}_{\perp} \cdot \frac{\vec{\nabla}_{\perp} \Psi}{R^2} \right) \vec{\nabla}\zeta \tag{6}$$

$$U = \left(\frac{R}{R_0}\right)^2 \vec{\nabla}_{\perp}^2 \Phi \tag{7}$$

$$P_* = \left(\frac{R}{R_0}\right)^{2\gamma} P \tag{8}$$

where R_0 is the major radius, $\zeta = R_0 \phi$, $\vec{\nabla}_{\perp} \equiv \frac{\partial}{\partial R} \vec{\nabla} R + \frac{\partial}{\partial z} \vec{\nabla} z$. The quantities U, Ψ and Φ denote the vorticity, poloidal flux and stream function, respectively. The energy integral of this reduced set of equations is given by

$$\frac{d}{dt} \int d\tau \left[\left(\frac{R}{R_0}\right)^2 | \vec{\nabla}\Phi |^2 + \left(\frac{R}{R_0}\right)^2 | \vec{\nabla}\Psi |^2 + \frac{P}{\gamma - 1} \right]$$

$$= - \int d\tau \left[\left(\frac{R}{R_0}\right)^2 \eta J^2 \right] + 2\pi R_0 E_w(t) I_p \ . \tag{9}$$

The first term in the l.h.s. represents the kinetic energy, the second one the magnetic energy, and the third one the internal energy. The first term in the r.h.s. is the energy dissipation. The electric field at the wall, $E_w(t)$, is obtained from eq.(9) by setting the total plasma current I_p constant.

Now we employ the coordinate system (r, θ, ζ) , in which the magnetic lines are straight. The radial coordinate r is defined by

$$r = \left(\frac{R}{R_0}\right)^2 \sqrt{g} \tag{10}$$

where $\sqrt{g}$ is Jacobian. The variables Ψ, J, Φ and P_* are Fourier expanded in θ and ζ directions:

$$\Psi(r,\theta,\zeta) = \sum_{m,n} \Psi_{m/n}(r) \exp i(m\theta - \frac{n}{R_0}\zeta) \tag{11}$$

where m and n denote the mode numbers in θ and ζ directions, respectively. The Fourier expanded equations are written as follows;

$$\frac{\partial \Psi_{m/n}}{\partial t} = [\Psi,\Phi]_{m/n} + \frac{B_0}{R_0} n \Phi_{m/n} + \eta J_{m/n} - E_{m/n} \tag{12}$$

$$\frac{\partial U_{m/n}}{\partial t} = [U,\Phi]_{m/n} + [J,\Psi]_{m/n} - \frac{R_0}{B_0} n J_{m/n} + [F,P]_{m/n} \tag{13}$$

$$\frac{\partial P_{*m/n}}{\partial t} = [\Phi,P_*]_{m/n} \tag{14}$$

where $[\Psi,\Phi]_{m/n}$ is defined by

$$[\Psi,\Phi]_{m/n} = \sum_{\substack{m=m'+m'' \\ n=n'+n''}} \frac{m'}{r} \left(\Psi_{m'/n'} \frac{d}{dr}\Phi_{m''/n''} - \Phi_{m'/n'} \frac{d}{dr}\Psi_{m''/n''} \right) . \tag{15}$$

Variables $J_{m/n}$ and $U_{m/n}$ take the form;

$$J_{m/n} = \frac{1}{r} \sum_{m=m'+m''} \left[\frac{d}{dr}\left(G^{rr}_{m'} \frac{d}{dr} \Psi_{m''/n} \right) - m'' \frac{d}{dr}\left(G^{r\theta}_{m'} \Psi_{m''/n} \right) \right.$$
$$\left. - m G^{r\theta}_{m'} \frac{d}{dr} \Psi_{m''/n} - m m'' G^{\theta\theta}_{m'} \Psi_{m''/n} \right] \tag{16}$$

$$U_{m/n} = \frac{1}{r} \sum_{m=m'+m''} \left[\frac{d}{dr}\left(H^{rr}_{m'} \frac{d}{dr} \Phi_{m''/n} \right) - m'' \frac{d}{dr}\left(H^{r\theta}_{m'} \Phi_{m''/n} \right) \right.$$
$$\left. - m H^{r\theta}_{m'} \frac{d}{dr} \Phi_{m''/n} - m m'' H^{\theta\theta}_{m'} \Phi_{m''/n} \right] . \tag{17}$$

Quantities F_m, G^{ij}_m and H^{ij}_m are defined by

$$\left(\frac{R}{R_0}\right)^2 = \sum_m F_m(r) \exp im\theta \tag{18}$$

$$r\, g^{ij} = \sum_m G^{ij}_m(r) \exp im\theta \tag{19}$$

$$r \left(\frac{R}{R_0}\right)^2 g^{ij} = \sum_m H^{ij}_m(r) \exp im\theta . \tag{20}$$

In this calculation the equation (14) for pressure is neglected because the pressure driven mode is not important in a low β plasma. Morever we neglect the toroidal effects. Even by this simplification, the essential mechanism of the major disruption can be described. We assume the resistivity is constant in time and set it to be

$$\eta(r) = E_w(t=0)/J(r,t=0) \ . \qquad (21)$$

The multi helicity calculation is carried out with up to 29 Fourier components and 200 equal-spacing radial meshes. The equations are solved by both the full-explicit and implicit-explicit predictor-corrector time integration schemes, and a good agreement between both cases is obtained. The time step for the former scheme, however, is restricted to be much small compared with that for the latter scheme.

3. Computational Results

3.1 Nonlinear Destabilization of 3/2 mode

We choose the q-profile as in Ref.1, $q(r)=1.38[1+(r/0.6)^8]^{1/4}$ and the magnetic Reynolds number $S=2\times10^4$ at q=2 surface. Almost the same behavior of the plasma as that of the ORNL calculation is recoverd, which is presented in the following figures (fig.1-7). Figure 1 (a and b) show the time evolution of magnetic island width obtained by the single-helicity and multi-helicity calculations, respectively. The single helicity calculation shows that the 2/1 and 3/2 modes are both unstable and the widths of the saturated islands are about 0.4 and 0.1, respectively. In contrast with the single-helicity calculation, the multi-helicity calclulation shows the rapid destabilization of 3/2 mode after the island of the 2/1 and 3/2 mode touch each other at $t \simeq 300$, due to the nonlinear interaction between modes with different helicities. The phase of the 5/3 and 7/4 modes are inverted several times at final stage of the disruption. The evolution of the kinetic and magnetic energies are shown in Fig.2 (a and b), respectively. Both the energies rapidly increase from the island-overlapping time ($t \simeq 300$). The time evolution of the growth rate of the magnetic energy is shown in Fig.3. The growth rate of the 2/1 mode is slowly decreasing function of time when the growth rates of the 3/2 and 5/3 modes begin to increase,which means that the 2/1 mode is in the Rutherford regime even after the time of the island overlapping. Figure 4 shows the time evolution of the one turn voltage, $V=[\frac{d}{dt}(E_k + E_M) - Q]/I_p$, where I_p is total plasma current, E_k and E_M are

In this calculation the equation (14) for pressure is neglected because the pressure driven mode is not important in a low β plasma. Morever we neglect the toroidal effects. Even by this simplification, the essential mechanism of the major disruption can be described. We assume the resistivity is constant in time and set it to be

$$\eta(r) = E_w(t=0)/J(r,t=0) \ . \qquad (21)$$

The multi helicity calculation is carried out with up to 29 Fourier components and 200 equal-spacing radial meshes. The equations are solved by both the full-explicit and implicit-explicit predictor-corrector time integration schemes, and a good agreement between both cases is obtained. The time step for the former scheme, however, is restricted to be much small compared with that for the latter scheme.

3. Computational Results

3.1 Nonlinear Destabilization of 3/2 mode

We choose the q-profile as in Ref.1, $q(r)=1.38[1+(r/0.6)^8]^{1/4}$ and the magnetic Reynolds number $S=2\times10^4$ at q=2 surface. Almost the same behavior of the plasma as that of the ORNL calculation is recoverd, which is presented in the following figures (fig.1-7). Figure 1 (a and b) show the time evolution of magnetic island width obtained by the single-helicity and multi-helicity calculations, respectively. The single helicity calculation shows that the 2/1 and 3/2 modes are both unstable and the widths of the saturated islands are about 0.4 and 0.1, respectively. In contrast with the single-helicity calculation, the multi-helicity calclulation shows the rapid destabilization of 3/2 mode after the island of the 2/1 and 3/2 mode touch each other at $t \simeq 300$, due to the nonlinear interaction between modes with different helicities. The phase of the 5/3 and 7/4 modes are inverted several times at final stage of the disruption. The evolution of the kinetic and magnetic energies are shown in Fig.2 (a and b), respectively. Both the energies rapidly increase from the island-overlapping time ($t \simeq 300$). The time evolution of the growth rate of the magnetic energy is shown in Fig.3. The growth rate of the 2/1 mode is slowly decreasing function of time when the growth rates of the 3/2 and 5/3 modes begin to increase,which means that the 2/1 mode is in the Rutherford regime even after the time of the island overlapping. Figure 4 shows the time evolution of the one turn voltage, $V=[\frac{d}{dt}(E_k + E_M) - Q]/I_p$, where I_p is total plasma current, E_k and E_M are

the kinetic and magnetic energies, and Q is the change in the rate of energy dissipation due to Joule heating. In this figure, V is normalized by $\eta B_t/\mu_0$. The negative voltage spike is observed is the figure. The order of magnitude of the voltage spike is in good agreement with experimental value. The helical flux contours for several modes with different helicities at the end of the calculation are shown in figure 5. The magnetic islands of the higher harmonics, such as the 8/5 or 13/7 modes, have also fairly large amplitude. In Fig.6, intersections of a single magnetic field line near the separatrix of the 2/1 island at the ζ=0 poloidal plane are plotted. This figure shows that the stochastic region develops during the interval(t=300∿400) and covers almost the plasma column at the final stage. The stochasticity can be investigated quantitatively by calculating the K-S entropy[5], which is shown in Fig.7. The evolution of the K-S entropy confirms the above result. The stochastic magnetic field in the plasma column enhances the heat loss and causes the rapid cooling of the plasma, which is observed in the soft X ray signals from the plasma center.

3.2 Effect of the Internal Disruption

Next, we calculate the nonlinear evolution of the 2/1 tearing mode in the presence of the 1/1 mode. The purpose of this calculation is to simulate destabilization of the 2/1 mode by the internal disruption through the flattening of the q-profile inside the q=1 surface. The initial q-profile in this case is $q(r)=0.9[1+(r/0.5)^{2\lambda}]^{1/\lambda}$, where $\lambda=2+2r^2$, and $S=2\times10^4$ at the q=1 surface (solid line in Fig.8). In this profile the islands of the 2/1 and 3/2 modes are saturated at relatively narrow width. The saturation width of the 2/1 and 3/2 islands ($W_{2/1}$ and $W_{3/2}$) estimated by using a Δ' code is $W_{2/1}$=0.109 and $W_{3/2}$=0.005 for the initial q-profile, and $W_{2/1}$=0.204, $W_{3/2}$=0.062 for the flattened q-profile (dashed line in Fig.8), respectively. There is no island overlapping between the 2/1 and 3/2 modes for the initial q-profile, while the island overlapping is expected for the flattened q-profile after the internal disruption. In order to investigate this possible enhancement of the 2/1 island width by the flattening of the current profile due to the internal disruption, the calculation is started with only the 2/1 mode, and the 1/1 mode is initiated at t=520 after the 2/1 island is saturated (Fig.9). The saturation width of the the 2/1 island at t=520 is $W_{2/1}$=0.07 which is a little smaller than the expected value. With the growth of the 1/1 mode, the 3/2 mode is produced by the coupling of the 1/1 and 2/1 modes, and the internal disruption occurs at

$t \cong 700$. After the internal disruption the q-profile inside of the q=1 surface is flattened and that outside of it is unchanged, (dotted line in Fig. ... indicate of the change of the q-profile, however, the island evolution of the 2/1 and 3/2 modes seems unchanged, even a long while after the internal disruption, i.e., $W_{2/1}=0.07$ and $W_{3/2}=0.014$ at t=970. These values are about 1/3 - 1/4 of those obtained by using the Δ' code and there is no assurance of island overlapping even if the calculation continues. There are other possibilities to initiate the major disruption. In Ref.6, we have shown that the size of the 2/1 island is strongly enhanced by the internal disruption due to the toroidal coupling. This result suggests that the major disruption is induced by the internal disruption in a toroidal plasma.

4. Conclusion and Discussion

We have studied the nonlinear evolution of tearing modes with different helicity in a cylindrical plasma and comfirmed that the major disruption is caused by the nonlinear destabilization of the 3/2 mode through the mode coupling with the 2/1 mode. And the evolution of the magnetic field topology has been precisely investigated. All these results support the mechanism of the major disruption, proposed by Waddel et al. The details of our results, however, are different from their results. Especially, in our simulation, the 2/1 mode is deeply in the Rutherford regime and its instantaneous growth rate is not affected even after the 3/2 mode is nonlinearly destabilized. This behavior of the 2/1 mode contradicts with the WKB theory. Therfore, the mechanism of the destabilization of the 3/2 mode remains unsolved

As for the effect of the internal mode on the major disruption, the flattening of the q-profile due to the internal disruption did not cause the enhancement of the 2/1 island width, in spite of the prediction of the major disruption by the Δ' calculation. The flattening occurs only inside of the q=1 surface and the q-profile is not affected near the 2/1 and 3/2 surfaces. Therefore, in order to expect the major disruption by the internal disruption, we have to take into account other effects, such as the toroidicity.

$t \cong 700$. After the internal disruption the q-profile inside of the q=1 surface is flattened and that outside of it is unchanged, (dotted line in Fig. ... shows the state of the change of the q-profile, however, the island evolution of the 2/1 and 3/2 modes seems unchanged, even a long while after the internal disruption, i.e., $W_{2/1}=0.07$ and $W_{3/2}=0.014$ at t=970. These values are about 1/3 - 1/4 of those obtained by using the Δ' code and there is no assurance of island overlapping even if the calculation continues. There are other possibilities to initiate the major disruption. In Ref.6, we have shown that the size of the 2/1 island is strongly enhanced by the internal disruption due to the toroidal coupling. This result suggests that the major disruption is induced by the internal disruption in a toroidal plasma.

4. Conclusion and Discussion

We have studied the nonlinear evolution of tearing modes with different helicity in a cylindrical plasma and comfirmed that the major disruption is caused by the nonlinear destabilization of the 3/2 mode through the mode coupling with the 2/1 mode. And the evolution of the magnetic field topology has been precisely investigated. All these results support the mechanism of the major disruption, proposed by Waddel et al. The details of our results, however, are different from their results. Especially, in our simulation, the 2/1 mode is deeply in the Rutherford regime and its instantaneous growth rate is not affected even after the 3/2 mode is nonlinearly destabilized. This behavior of the 2/1 mode contradicts with the WKB theory. Therfore, the mechanism of the destabilization of the 3/2 mode remains unsolved

As for the effect of the internal mode on the major disruption, the flattening of the q-profile due to the internal disruption did not cause the enhancement of the 2/1 island width, in spite of the prediction of the major disruption by the Δ' calculation. The flattening occurs only inside of the q=1 surface and the q-profile is not affected near the 2/1 and 3/2 surfaces. Therefore, in order to expect the major disruption by the internal disruption, we have to take into account other effects, such as the toroidicity.

Acknowledgments

The authors would like to thank Dr. M. Tanaka for his helpful discussion and continuing encouragement throughout the whole work. It is also a pleasure to thank Dr. Y. Obata for his encouragement during the whole work.

References

1) B. V. Waddel et al., Phys. Rev. Lett. 41 (1978) 1386.
2) B. V. Waddel et al., Phys. Fluids 22 (1979) 896.
3) B. Carreras et al., Phys. Fluids 23 (1980) 1811.
4) B. Carreras et al., Phys. Fluids 24 (1981) 66.
5) B. V. Chirikov, Phys. Reports 52 (1979) 263.
6) M. Azumi et al., "Internal disruption in high β_p tokamak", JAERI-M 9787 (1981).

Acknowledgments

The authors would like to thank Dr. M. Tanaka for his helpful discussion and continuing encouragement throughout the whole work. It is also a pleasure to thank Dr. Y. Obata for his encouragement during the whole work.

References

1) B. V. Waddel et al., Phys. Rev. Lett. 41 (1978) 1386.
2) B. V. Waddel et al., Phys. Fluids 22 (1979) 896.
3) B. Carreras et al., Phys. Fluids 23 (1980) 1811.
4) B. Carreras et al., Phys. Fluids 24 (1981) 66.
5) B. V. Chirikov, Phys. Reports 52 (1979) 263.
6) M. Azumi et al., "Internal disruption in high β_p tokamak", JAERI-M 9787 (1981).

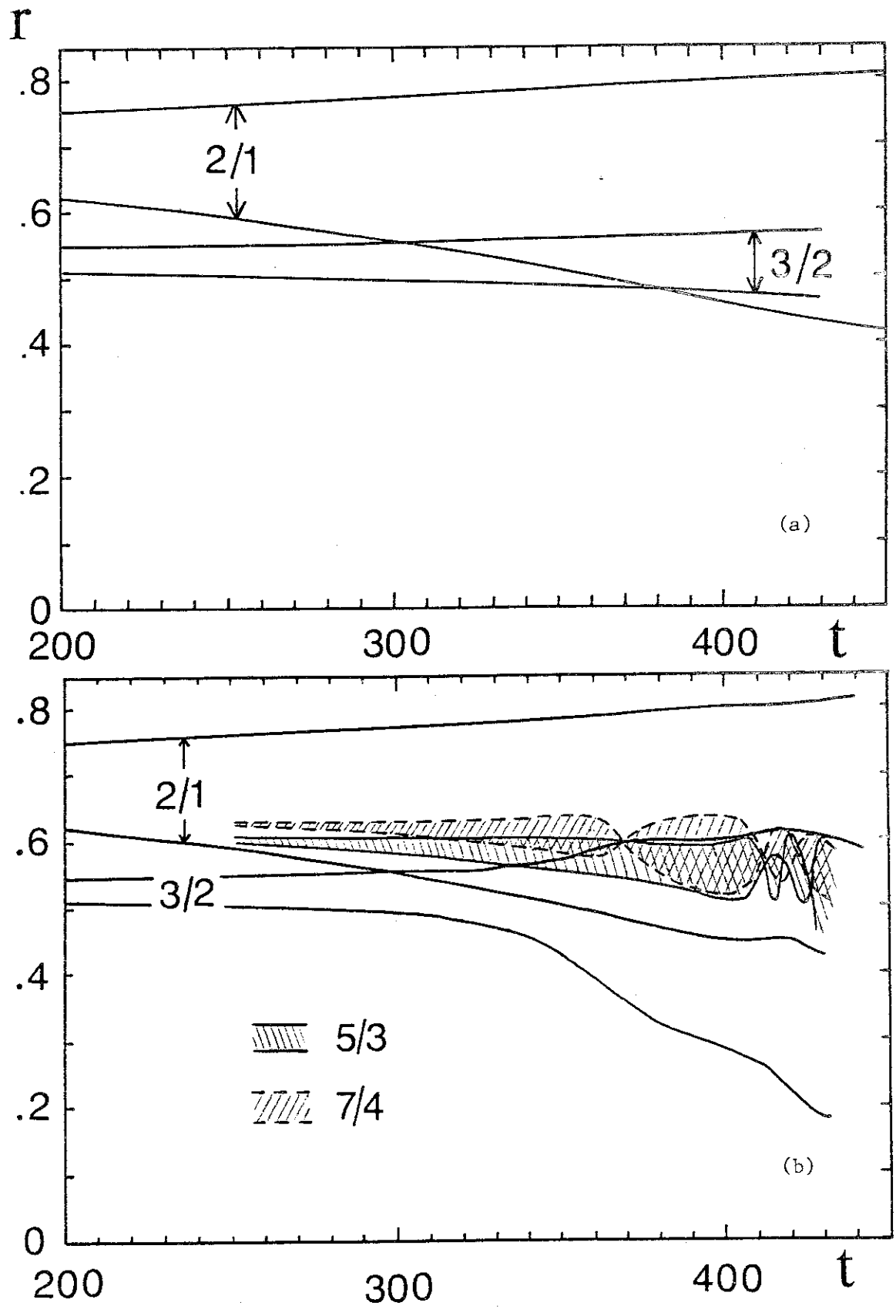

Fig.1 Time evolutions of the m/n mode magnetic island width for the case of (a) singl-helicity calculation and (b) multi-helicity calculation. The widths for both cases are the same before the island-overlapping time (t=300).

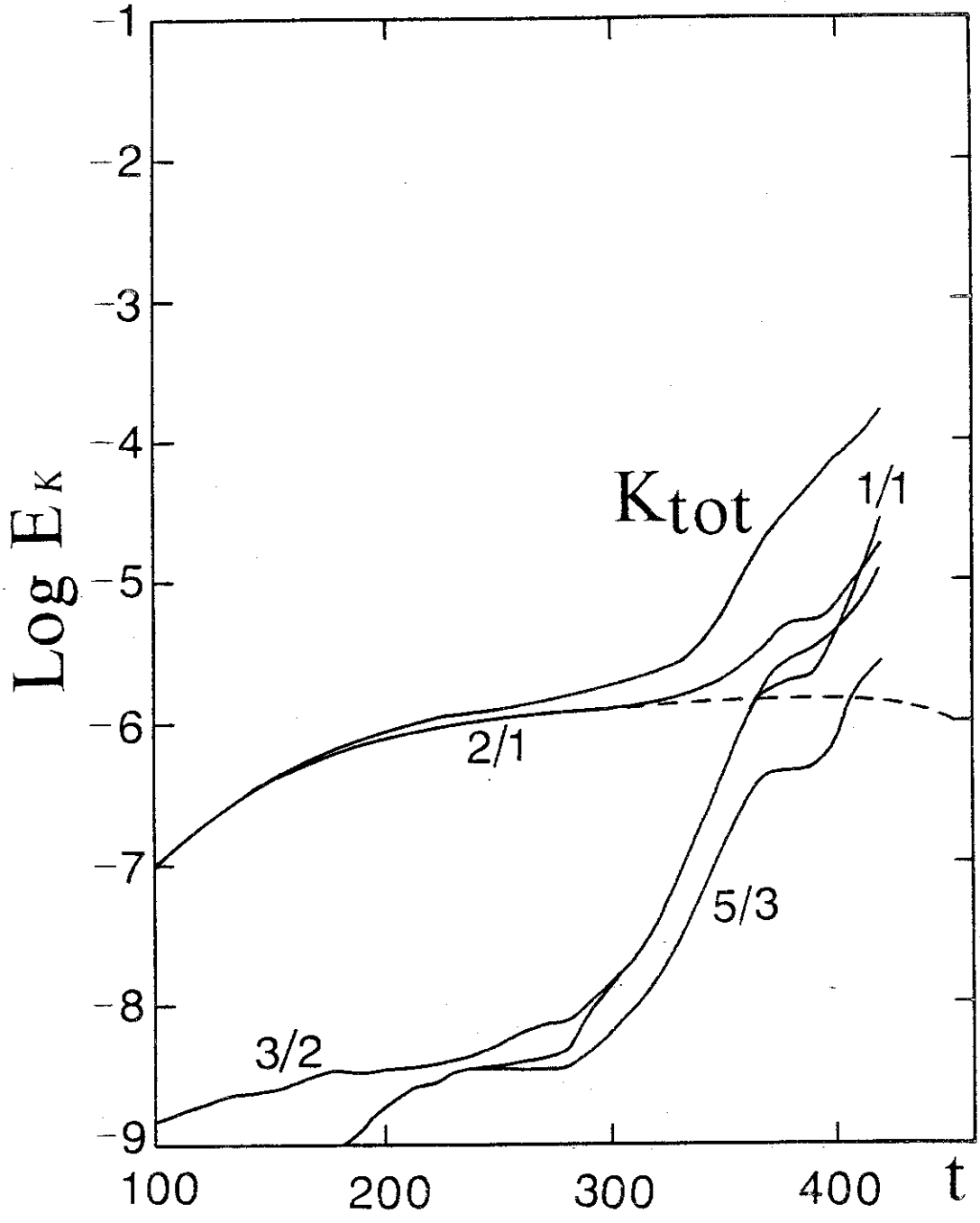

Fig.2(a) Time evolution of the kinetic energy in the case of multi-helicity calculation. Result for the single helicity calculation is shown by the dotted line.

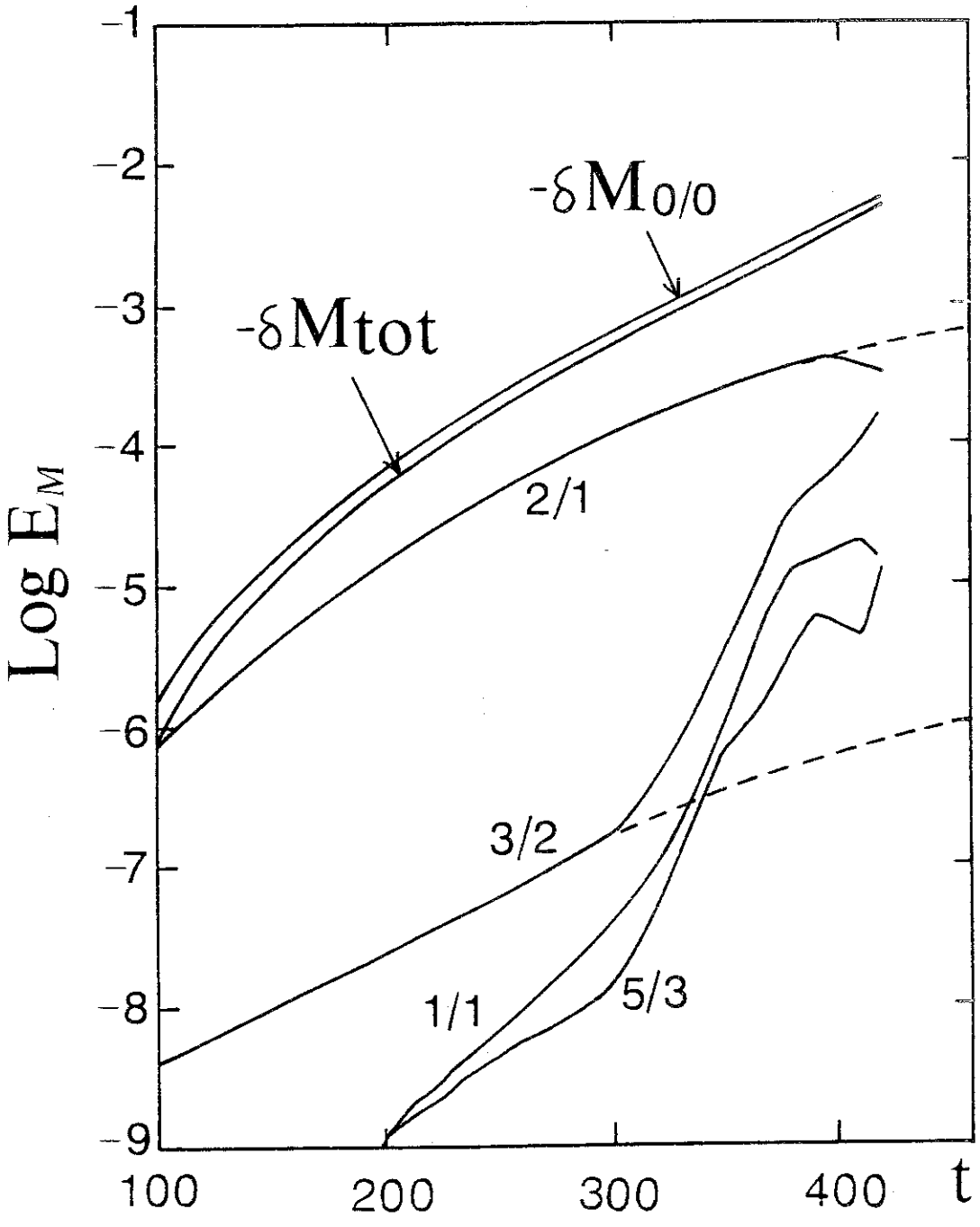

Fig.2(b) Time evolution of the magnetic energy in the case of multi-helicity calculation. Result for the single helicity calculation is shown by the dotted line.

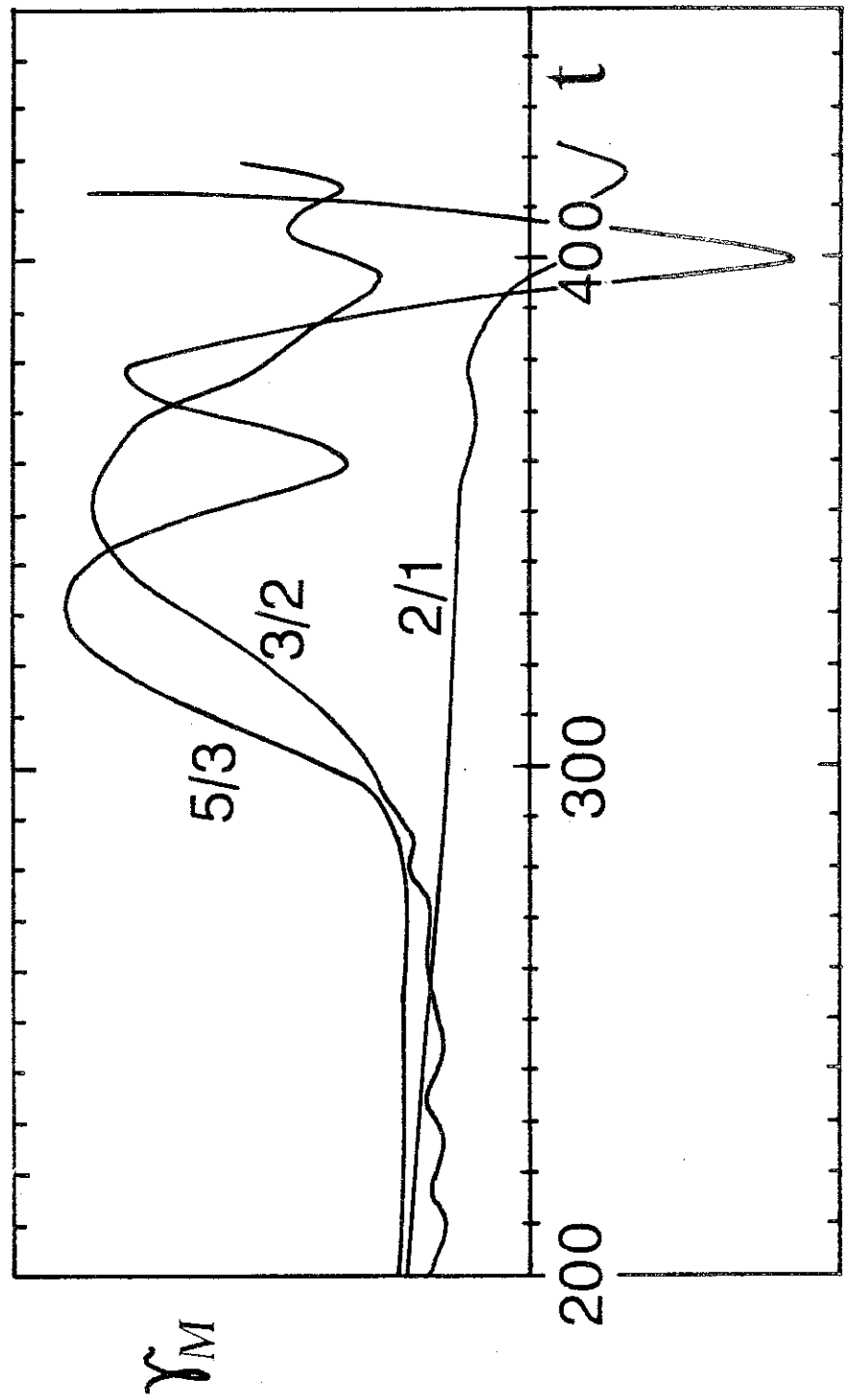

Fig.3 Instantaneous growth rates of the m/n magnetic energy. The growth rates of the 3/2 and 5/3 modes start to increase at the island-overlapping time (t=300), while the 2/1 mode remains in the Rutherford regime.

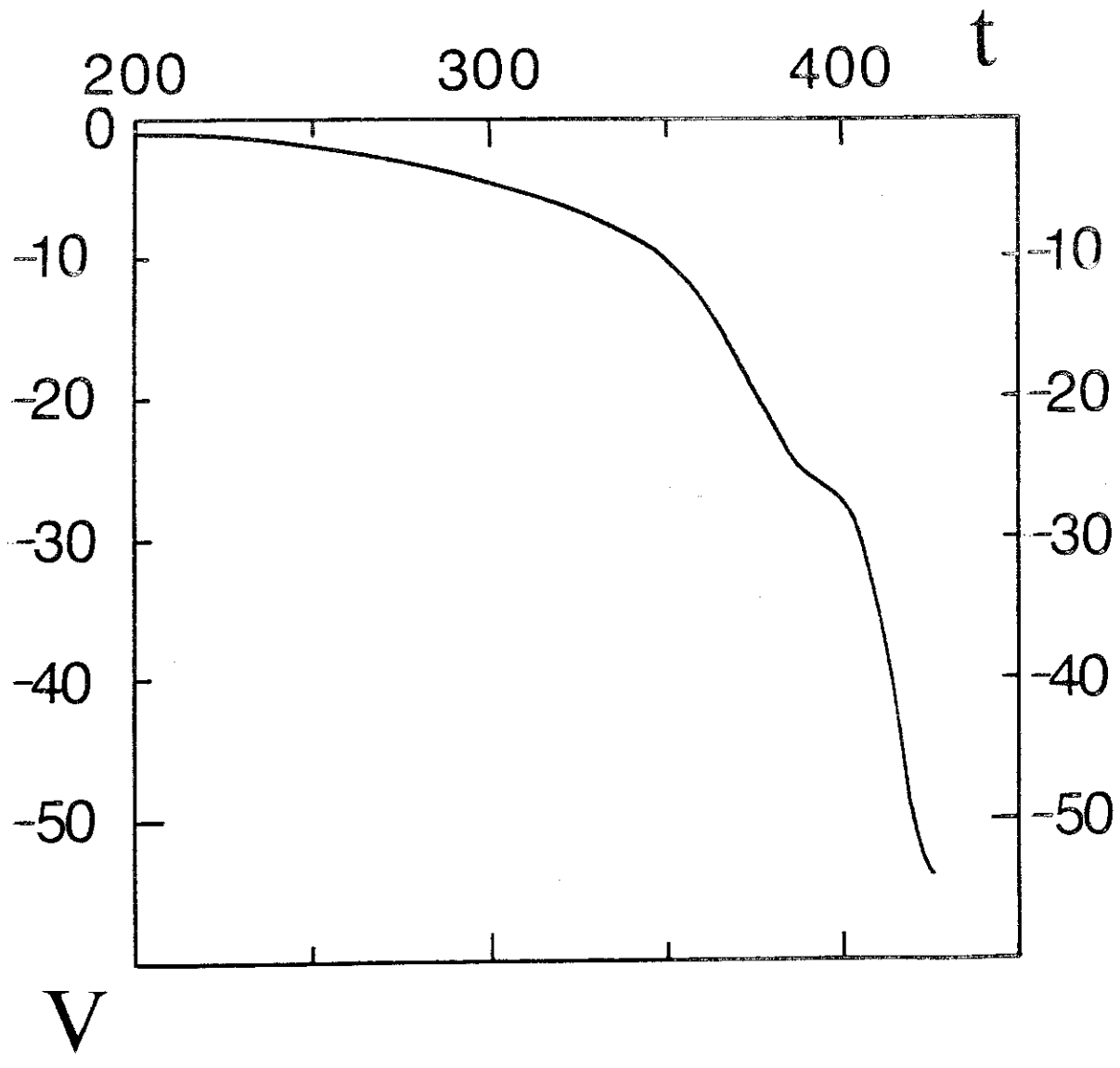

Fig.4 Time evolution of the one-turn voltage at the limiter.

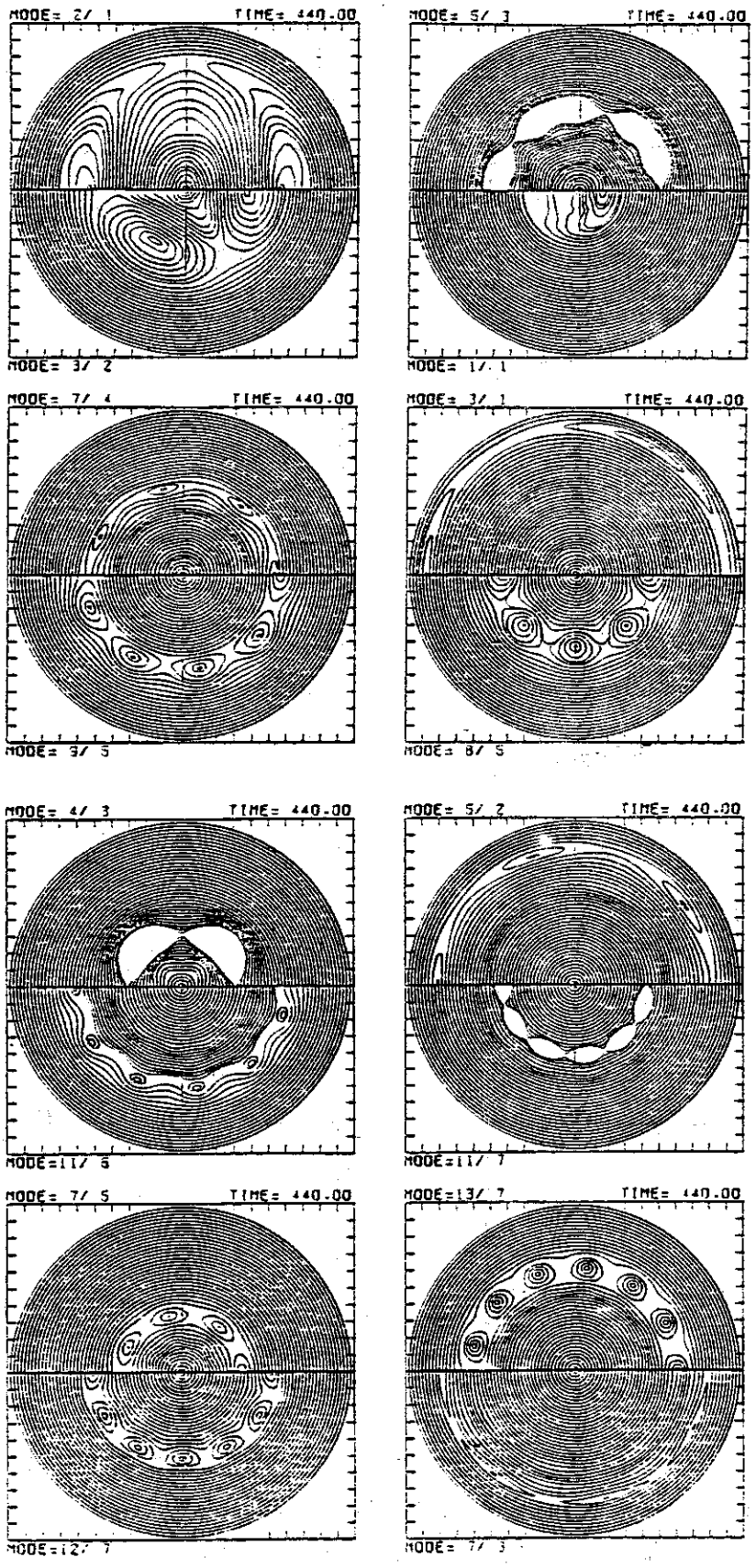

Fig.5 Helical flux contours of different helicities at the end of the calculation, t=440.

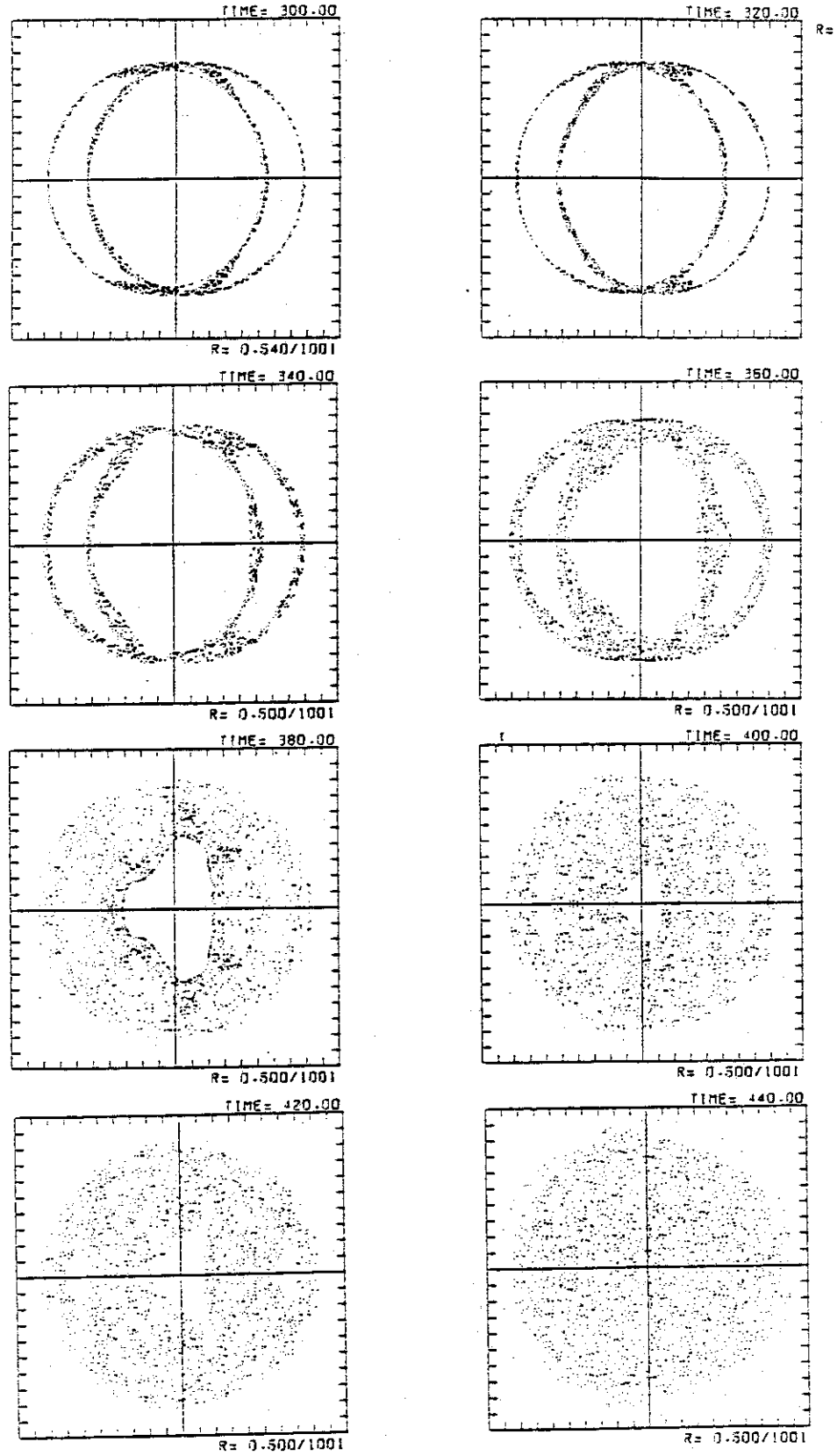

Fig.6 Trajectory of a magnetic field line, starting from a point on the separatrix of the 2/1 island. The cross-section at the poloidal plane ζ=0 is shown. Distinct structure of the 2/1 island is seen at the island-overlapping time t=300, while the trajectory is almost stochastic at t= 440.

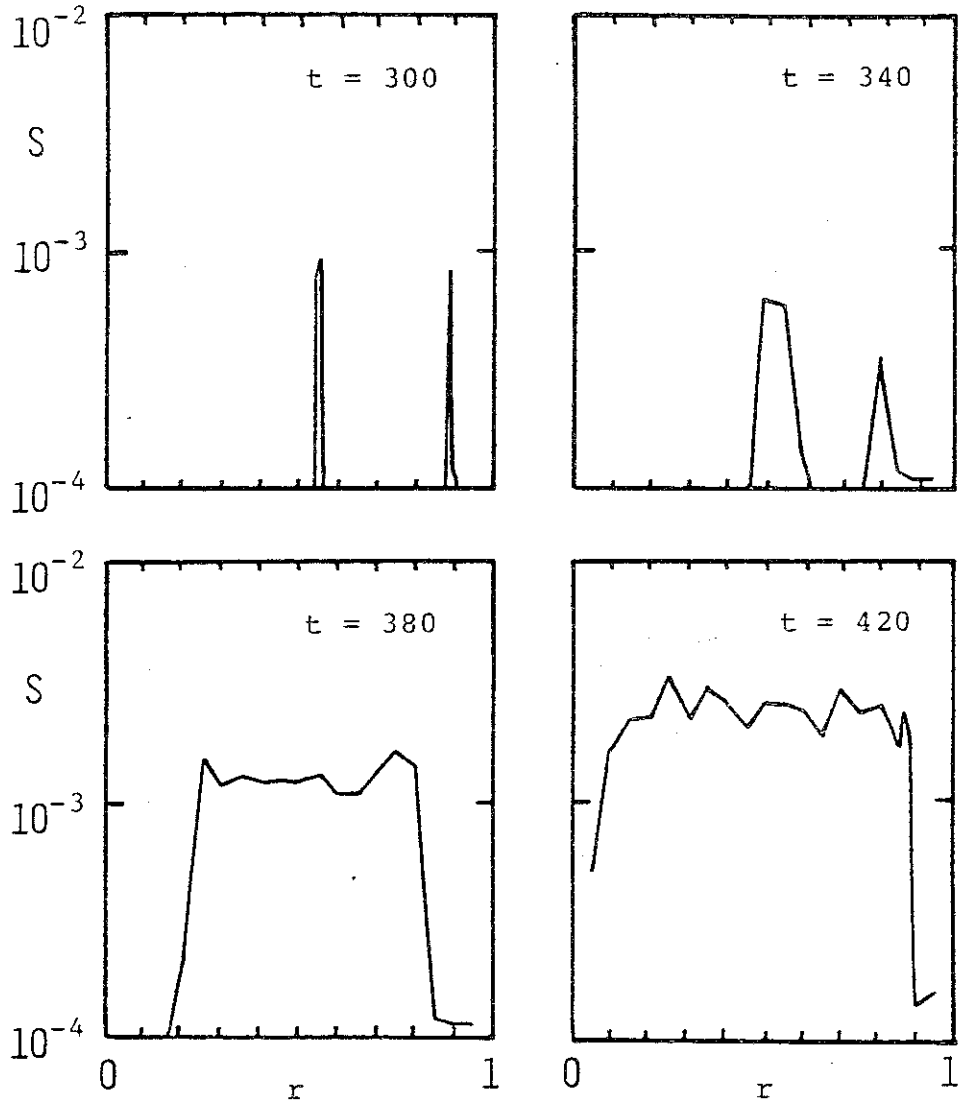

Fig.7 Space distributions of the K-S entropy of a magnetic field line at t= 300, 340, 380 and 420. The K-S entropy S is defined by

$$S = \lim_{N=\infty} \frac{1}{N} \sum_{n}^{N} \ln \ell_n$$

where n stands for an iteration serial number and ℓ_n is the distance between two field lines starting from neighbouring positions

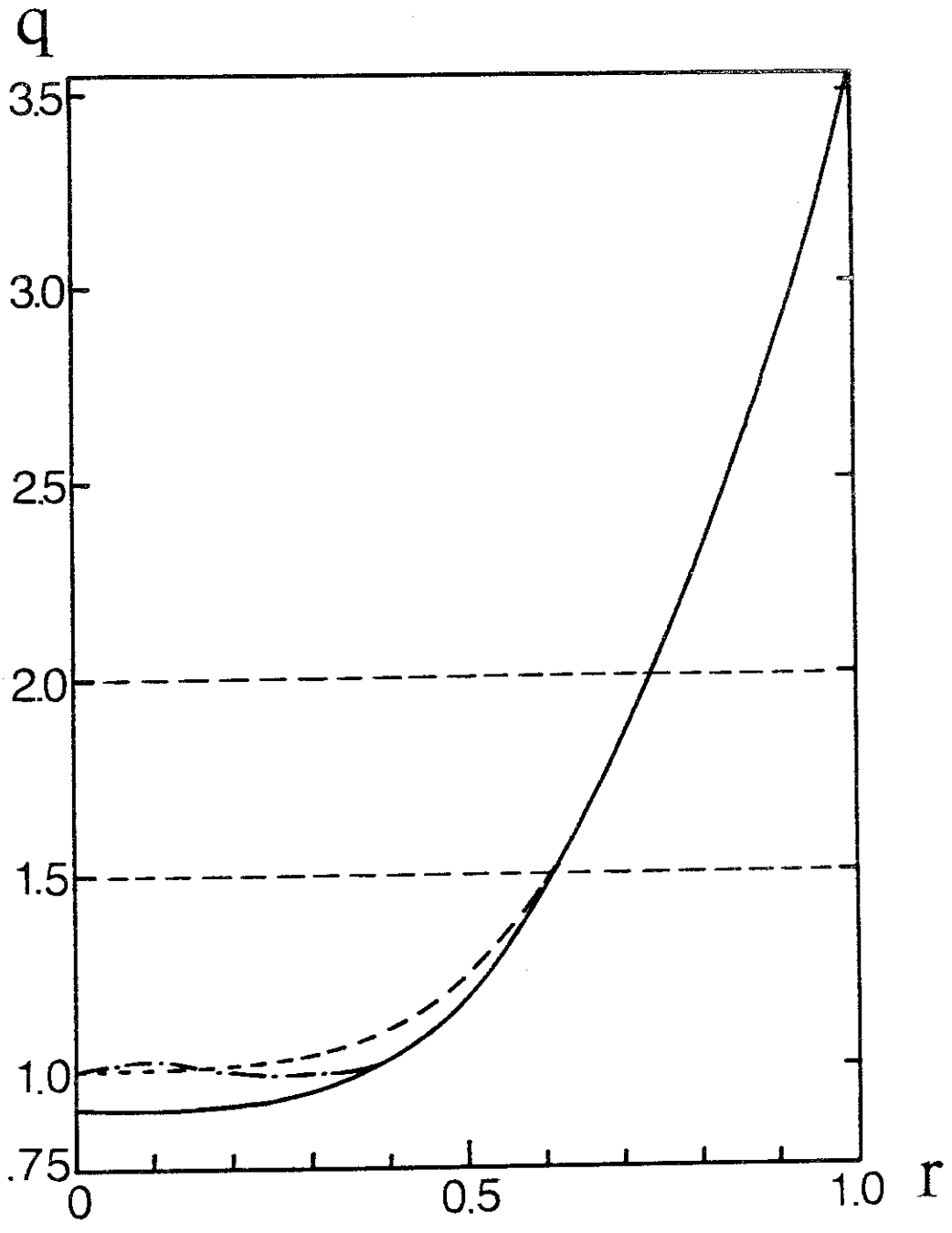

Fig.8 Profile of the safety factor q. The solid line denotes the initial q-profile (q_0=0.9 and q_a=3.6). The dotted line is the q-profile changed by the internal disruption. The model q-profile after the internal disruption for the Δ' calculation is shown by the dashed line.

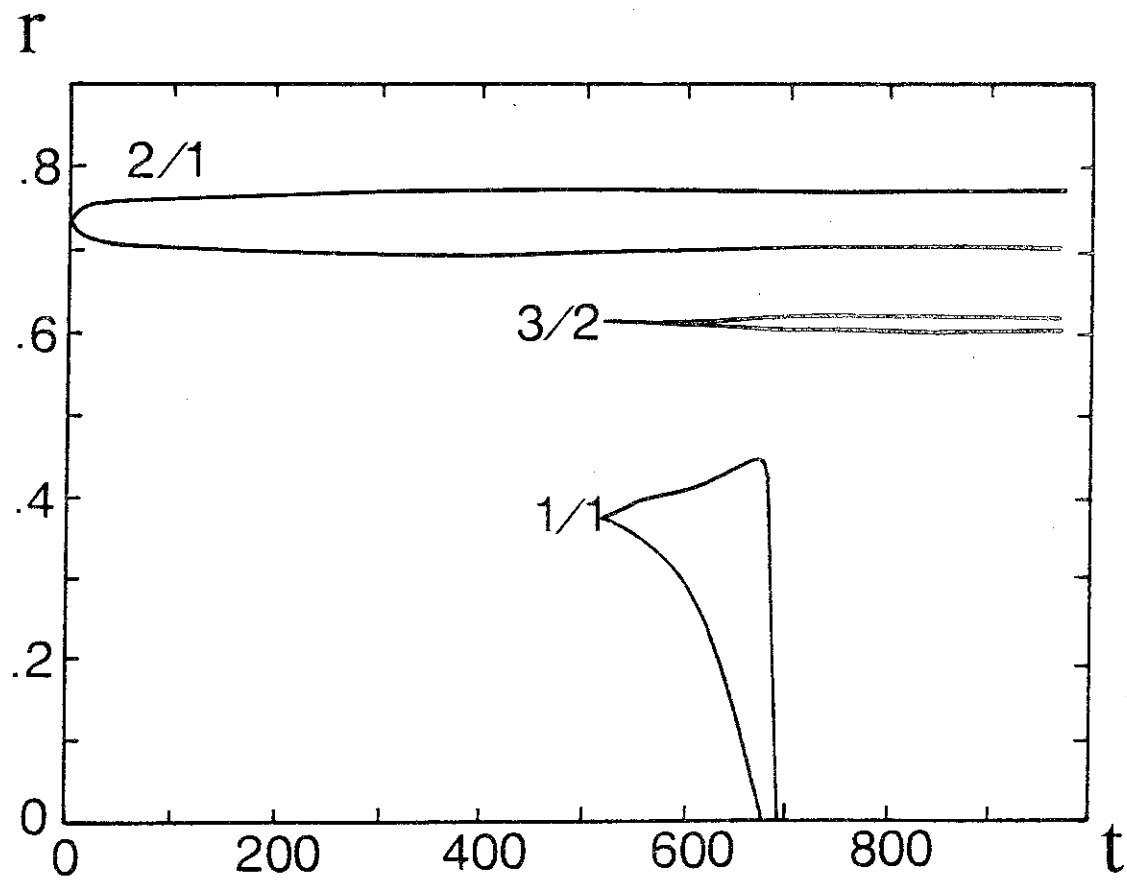

Fig.9 Time evolution of the magnetic island width. The result from t=0 to t=520 is obtained by the single-helicity calculation of the 2/1 mode. The 1/1 perturbation is added at t=520, and the evolution is simulated by the multi-helicity code. The internal disruption, which occurs at t=690, does not influence the 2/1 mode.